HIPPOCAMPUS 19:687–691 (2009)

RAPID COMMUNICATION

Hippocampal Long-Term Potentiation is Enhanced in Urethane-Anesthetized RGS2 Knockout Mice

R. Matthew Hutchison,[1,2] Peter Chidiac,[2] and L. Stan Leung[1,2]*

ABSTRACT: RGS2 is a member of the regulator of G-protein signaling (RGS) family and has been implicated in cellular mechanisms associated with neuronal plasticity. Long-term potentiation (LTP) of RGS2 knockout and wild-type mice was examined at the Schaffer collaterals to CA1 pathway in urethane-anesthetized mice in vivo to examine RGS2's possible role in the regulation of potentiation. As compared to wild-type mice, RGS2 knockouts demonstrated much stronger LTP of the extracellular population spikes at the somatic and dendritic layers in CA1 region and more pronounced LTP of the population excitatory postsynaptic current sink. Under baseline conditions, RGS2 knockouts showed lower paired-pulse facilitation of the excitatory postsynaptic potentials and associated current sinks in vivo as compared with wild-type mice. The data show for the first time that RGS2 deficient mice in vivo differ from wild-type mice in both short-term and long-term synaptic plasticity suggesting that RGS2 serves as a negative regulator of long-term synaptic plasticity. © **2009 Wiley-Liss, Inc.**

KEY WORDS: RGS; hippocampus; paired-pulse facilitation; excitatory current sink; population spike

INTRODUCTION

Regulator of G-protein signaling (RGS) proteins function as GTPase activating proteins and serve to accelerate the hydrolysis of GTP to the inactive GDP-bound state (Ross and Wilkie, 2000). Increased GTPase activity limits the duration of action of the dissociated Gα and Gβγ subunits, which are messenger signals for the various cellular functions mediated by activation of G-protein coupled receptors.

A member of the RGS family of proteins, RGS2 is unique in that it preferentially interferes with signals mediated via G_q and G_s alpha subunits while having relatively low potency toward G_i (Cladman and Chidiac, 2002; Roy et al., 2006). Functionally, RGS2 has been shown to modulate phospholipase C-β activity (Heximer et al., 1997), affect the activation of cAMP-gated calcium channels (Sinnarajah et al., 2001), reduce cAMP production by adenylyl cyclase (Sinnarajah et al., 2001; Roy et al., 2006), control experience-dependent brain development (Ingi and Aoki, 2002), and participate in the modulation and re-organization of neural circuits (Ingi et al., 1998).

Conflicting experimental results make it difficult to determine RGS2's role in neuronal functioning. It is suggested that RGS2 induction modifies the signaling properties of neurons by reducing the magnitude or duration of the G_q-dependent ligand-receptor systems as RGS2 mRNA is rapidly induced in hippocampal neurons in response to plasticity-inducing synaptic stimuli (Ingi et al., 1998). RGS2 upregulation is proposed to modulate G_q receptor-mediated release of intracellular calcium from inositoltrisphosphate-sensitive pools which is supported by the demonstration that a closely related protein, RGS4, inhibits calcium signaling by group I metabotropic glutamate receptors (mGluRs) (Saugstad et al., 1998). However, RGS2 knockout mice ($RGS2^{-/-}$) did not differ from heterogeneous controls ($RGS2^{+/-}$) with respect to LTP induced at the Schaffer-collaterals to CA1 synapses in vitro (Oliveira-Dos-Santos et al., 2000).

Because synaptic function and plasticity may differ in vivo and in vitro (Buckmaster and Schwartzkroin, 1995; Bliss et al., 2007), it is possible that RGS2's effect may not be apparent in a hippocampal slice preparation in vitro. The fact that endogenous RGS2 can attenuate G_q-dependent calcium increases suggests that RGS2 knockout mice may show enhanced calcium signaling via mGlu and other receptors. Thus, we hypothesized that RGS2 knockout mice would show increased LTP compared with wild-type controls, and we compared LTP at the apical dendritic synapses of CA1 in $RGS2^{-/-}$ and $RGS2^{+/+}$ mice under urethane anesthesia in vivo.

Average evoked potentials were recorded by a multichannel silicon probe and analyzed as current source density (CSD) (Fig. 1). CSD analysis reveals whether each unit volume (50 μm-thick slabs in this report) at one particular time shows a net inward current (sink) or outward current (source). For a laminated hippocampal CA1 area, each slab corresponds to a particular location on the dendrites and soma of the pyramidal cells that generate most of the extracellular potential.

CA3 stimulation activated the Schaffer collaterals and resulted in an excitatory current sink (ES) at the apical dendritic layer or stratum radiatum (RAD in

[1] **Graduate Program in Neuroscience, University of Western Ontario (UWO), London, Ontario, Canada;** [2] **Department of Physiology and Pharmacology, UWO**

Grant sponsor: Canadian Institutes of Health Research; Grant numbers: MOP 15685, IML 37987.

*Correspondence to: Dr. L. Stan Leung, Department Physiology and Pharmacology, University of Western Ontario, Medical Sciences Building Room 236, London, Ontario, N6A 5C1 Canada. E-mail: sleung@uwo.ca

Accepted for publication 19 January 2009
DOI 10.1002/hipo.20582
Published online 17 March 2009 in Wiley InterScience (www.interscience.wiley.com).

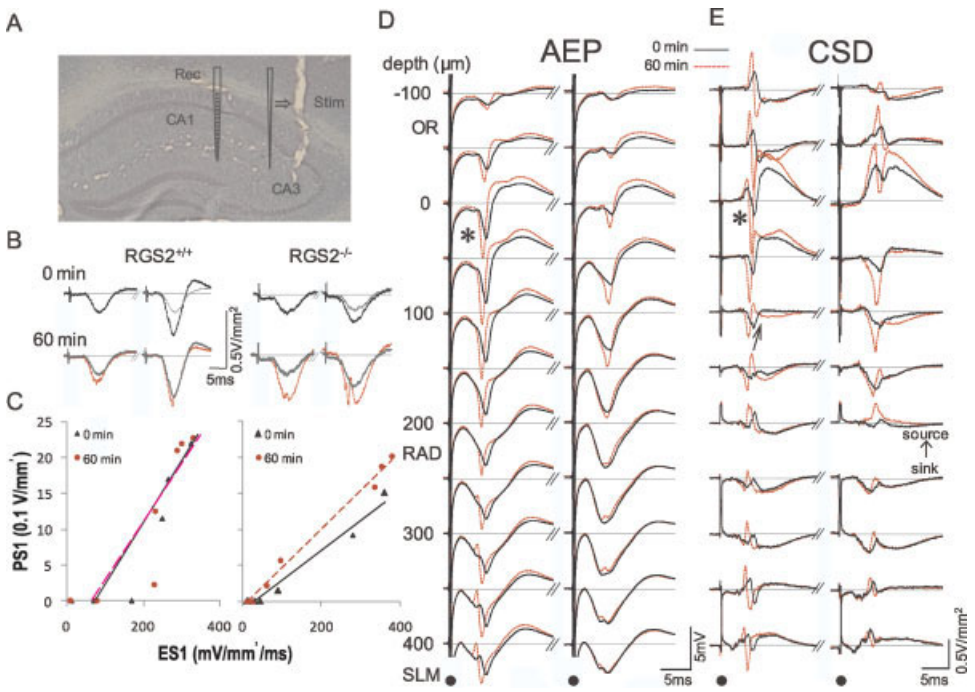

FIGURE 1. LTP in CA1 following a 100 Hz tetanic stimulation of the Schaffer collaterals. (A) Thionin-stained histological section that contained the track (⇒) of the stimulating electrode (Stim) in CA3 and a schematic of the 16-channel silicon recording probe (Rec) placed in ipsilateral CA1. (B) Baseline (0 min) shows greater paired-pulsed facilitation of the excitatory sink (ES) in wild-type (RGS2$^{+/+}$) mice than RGS2$^{-/-}$ mice (50 ms interpulse interval, ×1.5 ES threshold stimulus intensity; current source density (CSD) traces shown); the 1st pulse and 2nd pulse responses are overlaid on the right. At 60 min post-tetanus, CSD (dotted red traces) show LTP, when overlaid with the baseline (gray traces). (C) ES-PS (E-S) plots for the 1st pulse response, baseline (0 min) vs. 60 min post-tetanus, of representative wild-type and knockout mice. Best-fit linear regression lines were statistically different for the RGS2$^{-/-}$ mouse but not for the wild-type mouse. Profiles of (D) average evoked potentials (AEP) and (E) CSD of a representative RGS2$^{-/-}$ mouse, with baseline (black traces) overlaid on those recorded at 60 min post-tetanus (dashed red traces) to show potentiation of the ES and population spike (*). The 1st and 2nd stimulus pulses (stimulus artifacts labeled by filled circles) were separated by an interpulse interval of 50 ms. Relative depth (in μm from the cell layer, 0 μm) on the left; stratum oriens (OR), stratum radiatum (RAD), and stratum lacunosum-moleculare (SLM). The arrow represents the direction of propagation of the proximal population spike. [Color figure can be viewed in the online issue, which is available at www.interscience.wiley.com.]

Fig. 1E), which was associated with a population excitatory postsynaptic potential (pEPSP). At moderate to high stimulus intensity, a population spike sink (PS) rose from the ES. The PS latency was smallest at the proximal apical dendrites (150 μm depth in Fig. 1E), and it increased proximally toward the cell layer and basal dendrites (OR in Fig. 1E), and distally toward the distal apical dendrites. The increase in PS latency suggests propagation of the spike from the proximal apical dendrites to the basal and distal apical dendrites (Kloosterman et al., 2001).

In the baseline condition before LTP induction, RGS2$^{+/+}$ ($n = 9$) and RGS2$^{-/-}$ ($n = 8$) mice did not significantly differ ($P > 0.05$, Wilcoxon) in many measures of synaptic response (Table 1), including the threshold intensity that evoked a visually detectable ES response, the ES evoked by the first (ES1) and the second (ES2) pulse, and the amplitude of the population spike sink evoked by the first (PS1) and second (PS2) pulse. However, the ratio of ES2 to ES1 or paired-pulse facilitation (PPF) at 50 ms was significantly higher ($P < 0.01$, Wilcoxon) in wild-type than knockout mice, at both 1.5 and 2 times ES threshold stimulus intensities (Fig. 1B; Table 1). Similar PPF differences were found for the ratio of pEPSPs measured by their rising slopes (Table 1). In addition, the onset times of ES1 and PS1 were significantly earlier in knockout than wild-type mice (Table 1).

LTP was induced following tetanic stimulation (1-s train of 100 pulses at an intensity of 2× ES1 threshold) in both groups ($n = 7$ in each group). Repeated measures analysis of variance (ANOVA) of ES1 data (measured at 2× threshold) showed a significant time effect [$F(12,210) = 5.22$, $P < 0.0001$] but only a trend in the group effect [$F(1,13) = 4.52$, $P = 0.055$] (Fig. 2A,B). In contrast, PS1 (measured at a stimulus intensity that evoked 50–75% of the maximal PS1) showed significant time [$F(12,210) = 7.11$, $P < 0.0001$], group [$F(1,13) = 11.58$, $P < 0.01$], and group x time interaction [$F(15,180) = 4.15$, $P < 0.0001$] effects (Fig. 2C,D). Post hoc analysis clearly showed a stronger potentiation of PS1 in the RGS2 knockout as compared with wild-type mice (Fig. 2D). The PS2/PS1 or ES2/ES1 ratios did not show any significant change following tetanic stimulation in knockout or wild-type mice.

TABLE 1.

Baseline Measures of Wild-Type RGS2$^{+/+}$ and RGS2 Knockout RGS2$^{-/-}$ Mice

	RGS2$^{+/+}$ (n = 9)	RGS2$^{-/-}$ (n = 8)
Threshold intensity (μA)	46 ± 3	46 ± 5
ES1 slope at 2× threshold (mV/mm^2/ms)	99 ± 13	118 ± 41
ES2 slope at 2× threshold (mV/mm^2/ms)	200 ± 35	182 ± 68
Maximal ES1 slope (mV/mm^2/ms)	222 ± 23	279 ± 55
ES2/ES1 ratio at 1.5× threshold	1.79 ± 0.1	1.25 ± 0.1*
ES2/ES1 ratio at 2× threshold	1.94 ± 0.1	1.53 ± 0.1*
pEPSP2/pEPSP1 ratio at 1.5× threshold	1.87 ± 0.12	1.27 ± 0.15*
pEPSP2/pEPSP1 ratio at 2× threshold	1.97 ± 0.11	1.49 ± 0.14**
Maximal PS1 (mV/mm^2)	867 ± 157	1030 ± 191
PS2/PS1 ratio at 50% PS1 maximum	1.51 ± 0.2	1.47 ± 0.5
ES1 onset at 6× threshold (ms)	5.6 ± 0.4	4.4 ± 0.2***
PS1 onset at 6× threshold (ms)	9.7 ± 0.3	8.1 ± 0.2***

Values shown are mean ± SEM. Excitatory sink following the 1st (ES1) and 2nd pulse (ES2), and population excitatory postsynaptic potential following the 1st pulse (pEPSP1) and 2nd pulse (pEPSP2), was measured as a rising slope of the event recorded at the CA1 apical dendrites. Stimulus intensities are stated as number of times of ES1 threshold. Population spike sink (PS1 and PS2 following the 1st and 2nd pulse, respectively) was measured as the amplitude of the negative sink transient at the CA1 cell body layer, at a stimulus intensity that evoked 50–75% of the maximal PS1. Maximal ES or PS measures were taken at the CA3 stimulus intensity that evoked the respective maximal response (< 600 μA). *$P < 0.01$, **$P < 0.05$, ***$P < 0.001$, Wilcoxon, difference between RGS2 $^{+/+}$ and RGS2$^{-/-}$ groups.

ES-PS (E-S) potentiation is shown as an upward shift of the PS1 amplitude graph as a function of the ES1 slope (Fig. 1C). The ES-PS relation during baseline, and at 60 min post-tetanus, were fitted by linear regression (all fits except in one knockout mouse showed $R^2 > 0.6$) and then compared using an analysis of covariance (ANCOVA). Four of seven knockout mice, but none of the seven wild-type mice, showed E-S potentiation indicated by a significant change in the regression lines; the proportion of mice with E-S potentiation was higher in the knockout than the wild-type group ($P < 0.05$, Chi-square test).

This is the first report that RGS2$^{-/-}$ mice, compared with wild-type controls, show an enhanced LTP but a reduced PPF of the Schaffer collateral evoked excitation in CA1. A previous study reported no difference in the in vitro LTP of the Schaffer collaterals between RGS2$^{-/-}$ and wild-type mice (Oliveira-Dos-Santos et al., 2000). Han et al. (2006) reported a larger PPF at autapses in hippocampal neuronal cultures deficient in RGS2. PPF is regarded as a presynaptic mechanism, and the decreased PPF in RGS2$^{-/-}$ as compared with wild-type mice in vivo reported here suggests that a higher presynaptic release probability in RGS2$^{-/-}$mice. Differences in onset latency of ES1 and PS1 between RGS2$^{-/-}$ and RGS2$^{+/+}$ mice were unexpected, and may suggest more synchronous activation and/or faster conduction velocity of the Schaffer collaterals in RGS2$^{-/-}$ mice.

Differences in LTP have been reported between in vitro and intact animals in vivo, in part because of a relative lack of inhibition in vitro (Buckmaster and Schwartzkroin, 1995). Disinhibition is known to increase the magnitude of LTP in CA1 in vivo (Kaibara and Leung, 1993). The preparation of in vitro slices may remove the normal modulation and inhibitory control of LTP and obscure the differences in LTP between knockout and wild-type mice in vivo. The intact subcortical innervation of the hippocampus in vivo (Amaral and Lavenex, 2007), in particular cholinergic afferents from the medial septal area, may provide strong activation of muscarinic receptors during tetanic stimulation. RGS2 was reported to bind to M1 receptors (Bernstein et al., 2004) and decrease M1 receptor activation that contributed to Schaffer collateral LTP induced during walking in rats (Doralp and Leung, 2008). However, whether disinhibition or M1 receptors are involved in enhancement of LTP of RGS2$^{-/-}$ mice remains to be studied.

Oliveira-Dos-Santos et al., (2000) reported normal spatial learning despite reduced dendritic spine density in CA1 hippocampal neurons and decreased pEPSPs vs. presynaptic volley amplitude in RGS2$^{-/-}$ mice. The dendritic spine loss was not shown in a subsequent study (Han et al., 2006). Although enhanced LTP and learning are often correlated, this is not always the case and impaired or no change in spatial memory has been reported in some transgenic strains of mice (Jun et al., 1998; see Bliss et al., 2007 for review). RGS2 deficiency may still manifest itself in other learning tasks yet to be investigated.

Metabotropic glutamatergic receptor (mGluR) regulation may account for the differences in LTP of the PSs in wild-type and RGS2$^{-/-}$ mice. An mGluR agonist decreased spike afterhyperpolarization (AHP), increased single cell excitability, decreased the threshold of LTP, enhanced E-S potentiation, and induced LTP by itself (Breakwell et al., 1996; Cohen et al., 1999). Activation of mGluRs, through the G_q-mediated and thus possibly RGS2-sensitive release of Ca^{2+} from internal stores, may function as LTP "threshold boosters" and contribute to the magnitude and longevity of the LTP induced by a weak tetanus (Wilsch et al., 1998). The relatively weak LTP of ES1 (~ 25% at 1 h) in the wild-type mice may suggest that the tetanization strength used in this study was weak. We suggest that the lack of RGS2 in knockout mice may allow a prolonged activation of mGluRs that enhances LTP by releasing Ca^{2+} from internal stores and increases excitability of CA1 pyramidal cells by decreasing AHP or GABAergic inhibition. The findings here suggest a role of RGS2 as a negative regulator of LTP of spike output, but the cellular mechanisms, including a possible modulation of mGluRs, remain to be studied.

DETAILED METHODS

RGS2$^{-/-}$ mice were generated using the protocol established by Roy et al. (2006). They were provided with normal food and water ad libitum and subjected to a standard light/dark cycle. The study was approved by an Animal Use Subcommit-

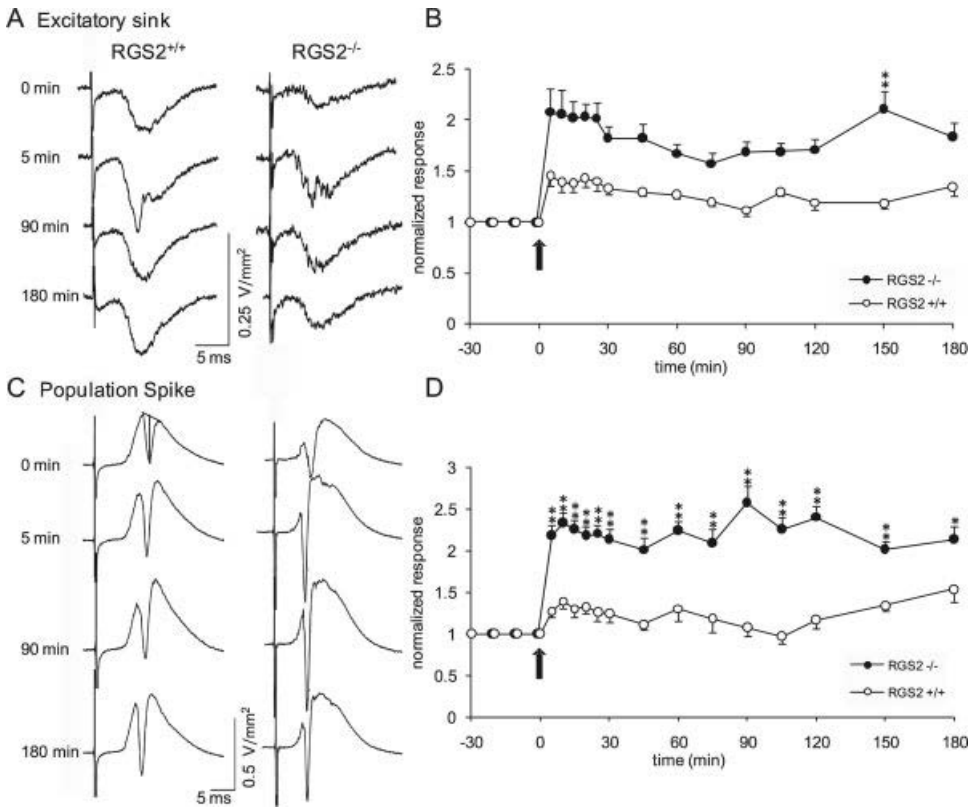

FIGURE 2. RGS2$^{-/-}$ mice demonstrate increased LTP following a tetanic (100 Hz) stimulation of the Schaffer collateral pathway compared with wild-type RGS2$^{+/+}$ controls. (A) Representative traces of first-pulse apical excitatory sink (ES1) at the apical dendritic layer, following ×2 ES1 threshold stimulation, at 0, 5, 90, and 180 min after tetanus, for wild-type (RGS2$^{+/+}$) and knockout (RGS2$^{-/-}$) mice. (B) ES1 was potentiated in both groups ($N = 7$ each); the baseline before tetanus was normalized to one in each experiment, and tetanus was delivered at time zero (↑). Error bars represent one SEM. (C) Representative traces of current source density at the CA1 cell layer, showing the first-pulse population spike sink (PS1) evoked by a stimulus intensity that evoked ∼50–75% of the maximal PS1 amplitude; layout same as (A). (D) RGS2$^{-/-}$ mice show more pronounced potentiation of PS1 than wild-type mice. *$P < 0.05$, **$P < 0.01$: significant difference between groups, Newman-Keuls post hoc test following a significant ANOVA.

tee at the University of Western Ontario, following guidelines of the Canadian Council on Animal Care.

Eight RGS2 knockout [weight: 26.6 ± 0.5 g, age: 4.25 ± 0.2 months; mean ± standard error of the mean (SEM)] and nine wild-type (28.9 ± 0.9 g, 4.06 ± 0.2 months) male mice were used. Mice did not significantly differ in terms of age or weight ($P > 0.05$, Wilcoxon). Animals were anesthetized with urethane (1 g/kg i.p.) and placed in a stereotaxic apparatus. Procaine (4%) was applied to both the inner ear and the scalp as a local anesthetic. Atropine methyl nitrate was administered (9 mg/kg i.p.) to reduce airway secretions. Animal body temperature was maintained between 36.5°C and 37°C via a feedback controlled rectal probe and heating pad. A 16-channel silicon recording probe (NeuroNexus, Ann Arbor, MI) was positioned in the CA1 area at P 2.2, L 1.4 (with respect to bregma; Fig. 1A; Paxinos and Franklin, 2001). The probe had 16 recording sites spaced 50 μm apart on a vertical shank. A stimulating electrode (125 μm Teflon-insulated steel wire) was placed in CA3 at P 2.2, L 2.5, at a depth (typically 2.3–2.5 mm below the skull surface) that was optimized to evoke the largest response at the apical dendritic synapses of CA1. Constant current paired-pulse stimuli (0.2 ms pulse duration), separated by 50 ms, were delivered once every 15 s, through an S88 stimulator and PSIU6 photo-isolated stimulus isolation unit (Astro-Med/Grass Instrument, RI), and triggered by a pulse generator (Master-8, A.M.P.I., Israel). Stainless steel screws in the frontal and occipital skull served as the stimulus anode and reference, respectively.

The multichannel signals were amplified 250×, filtered from 1 Hz–10 kHz and digitized at 24.4 KHz per channel by a preamplifier and digital processing base unit (Medusa Base Station RA16, Tucker-Davis Technologies, FL). For most animals, the responses to a low and a high intensity test-stimulus (average of 4 sweeps each, averaged successively) were used to establish a stable baseline. The low stimulus intensity was set at 2× ES threshold that typically did not evoke a PS during baseline. The high stimulus intensity evoked a PS of 50–75% of its maximum amplitude. After a stable baseline was recorded for at least 30 min (SEM to mean ratio <0.1 for ES1), a 1-s stimulation train of 100 Hz (tetanus) was delivered at 2× ES threshold intensity. Recordings were made for 3 h following the tetanus. Input-output response curves (1–6× ES threshold stimulus intensities) were generated before, and at 60, 120, and

180 min after the tetanus. Two wild-type and one knockout mouse were removed from the LTP analyses due to the induction of long-term depression.

One-dimensional CSD (z, t) as a function of depth (z) and time (t) was calculated by a second-order differencing formula (Leung, 1990),

$$\mathrm{CSD}(z,t) = \sigma[2\Phi(z,t) - \Phi(z+\Delta z,t) - \Phi(z-\Delta z,t)]/(\Delta z)^2$$

where Φ (z, t) is the potential at depth z and time t, and Δz is the spacing (50 μm) between adjacent electrodes on the 16-channel probe; no spatial smoothing of the CSDs was necessary (Leung, 1990). The conductivity σ was assumed to be constant and the CSDs were reported in units of V/mm^2 (Fig. 1D,E).

The CA1 cell layer was determined as the recording site that showed a near-maximal PS amplitude rising from the current source that accompanied an apical-dendritic excitation (Kloosterman et al., 2001). The peak amplitude of the PS was determined at the CA1 cell layer by the maximal vertical distance from the negative spike trace to the tangent line drawn between the positive peaks before and after the negative spike peak (Fig. 2C). ES or pEPSP was measured by the maximal slope over a 1 ms duration, before the onset of the PS.

At the end of each experiment, the stimulating electrode position was marked by a lesion with DC current of 1 mA for 1–2 s. Animals were perfused with saline and 4% formaldehyde, and the fixed, excised brains were sliced into 40 μm thick coronal sections and stained with thionin to locate the sites of recording and stimulating electrodes. The nonparametric Wilcoxon signed rank test and 2-factor (group x time) repeated measures ANOVA were used for group comparisons.

Acknowledgments

The authors would like to thank Pascal Peloquin for his technical assistance and Dr. Caroline Nunn for breeding the wild-type and $RGS2^{-/-}$ mice.

REFERENCES

Amaral D, Lavenex P. 2007. Hippocampal neuroanatomy. In: Anderson P, Morris R, Amaral D, Bliss T, O'Keefe J, editors. The Hippocampus Book. New York: Oxford University Press. pp 37–114.

Bernstein LS, Ramineni S, Hague C, Cladman W, Chidiac P, Levey AI, Hepler JR. 2004. RGS2 binds directly and selectively to the M1 muscarinic acetylcholine receptor third intracellular loop to modulate Gq/11 signaling. J Biol Chem 279:21248–21256.

Bliss TVP, Collingridge G, Morris RM. 2007. Synaptic plasticity in the hippocampus. In: Anderson P, Morris R, Amaral D, Bliss T, O'Keefe J, editors. The Hippocampus Book. New York: Oxford University Press. pp.343–474.

Breakwell NA, Rowan MJ, Anwyl R. 1996. Metabotropic glutamate receptor dependent EPSP and EPSP-spike potentiation in area CA1 of the submerged rat hippocampal slice. J Neurophysiol 76:3126–3135.

Buckmaster PS, Schwartzkroin PA. 1995. Interneurons and inhibition in the dentate gyrus of the rat in vivo. J Neurosci 15:774–789.

Cladman W, Chidiac P. 2002. Characterization and comparison of RGS2 and RGS4 as GTPase-activating proteins for m2 muscarinic receptor-stimulated G(i). Mol Pharmacol 62:654–659.

Cohen AS, Coussens CM, Raymond CR, Abraham WC. 1999. Long-lasting increase in cellular excitability associated with the priming of LTP induction in rat hippocampus. J Neurophysiol 82:3139–3148.

Doralp S, Leung LS. 2008. Cholinergic modulation of hippocampal CA1 basal-dendritic long-term potentiation. Neurobiol Learn Mem 90:382–388.

Han J, Mark MD, Li X, Xie M, Waka S, Rettig J, Herlitze S. 2006. RGS2 determines short-term synaptic plasticity in hippocampal neurons by regulating $G_{i/o}$-mediated inhibition of presynaptic Ca^{2+} channels. Neuron 51:575–486.

Heximer SP, Watson N, Linder ME, Blumer KJ, Hepler JR. 1997. RGS2/G0S8 is a selective inhibitor of G_q α14393.

Ingi T, Aoki Y. 2002. Expression of RGS2, RGS4 and RGS7 in the developing postnatal brain. Eur J Neurosci 15:929–936.

Ingi T, Krumins AM, Chidiac P, Brothers GM, Chung S, Snow BE, Barnes CA, Lanahan AA, Siderovski DP, Ross EM, Gilman AG, Worley PF. 1998. Dynamic regulation of RGS2 suggests a novel mechanism in G-protein signaling and neuronal plasticity. J Neurosci 18:7178–7188.

Jun K, Choi G, Yang SG, Choi KY, Kim H, Chan GC, Storm DR, Albert C, Mayr GW, Lee CJ, Shin HS. 1998. Enhanced hippocampal CA1 LTP but normal spatial learning in inositol 1,4,5-trisphosphate 3-kinase(A)-deficient mice. Learn Mem 5:317–330.

Kaibara T, Leung LS. 1993. Basal versus apical dendritic long-term potentiation of commissural afferents to hippocampal CA1: A current-source density study. J Neurosci 13:2391–2404.

Kloosterman F, Peloquin P, Leung LS. 2001. Apical and basal orthodromic population spikes in hippocampal CA1 in vivo show different origins and patterns of propagation. J Neurophysiol 86:2435–2444.

Leung LS. 1990. Field potentials in the central nervous system—Recording, analysis and modeling. In: Boulton AA, Baker GB, Vanderwolf CH, editors. Neurophysiological Techniques. Applications to Neural Systems (NeuroMethods, Vol 15). Clifton, NJ: Humana. pp 277–312.

Oliveira-Dos-Santos AJ, Matsumoto G, Snow BE, Bai D, Houston FP, Whishaw IQ, Mariathasan S, Sasaki T, Wakeham A, Ohashi PS, Roder JC, Barnes CA, Siderovski DP, Penninger JM. 2000. Regulation of T cell activation, anxiety, and male aggression by RGS2. Proc Natl Acad Sci USA 97:12272–12277.

Paxinos G, Franklin KB. 2001. The Mouse Brain in Stereotaxic Coordinates, 2nd Edition. Burlington, MA: Elsevier Science.

Ross EM, Wilkie TM. 2000. GTPase-activating proteins for heterotrimeric G proteins: Regulators of G protein signaling (RGS) and RGS-like proteins. Annu Rev Biochem 69:795–827.

Roy AA, Nunn C, Ming H, Zou MX, Penninger J, Kirshenbaum LA, Dixon SJ, Chidiac P. 2006. Up-regulation of endogenous RGS2 mediates cross-desensitization between G_s and G_q signaling in osteoblasts. J Biol Chem 281:32684–32693.

Saugstad JA, Marino MJ, Folk JA, Hepler JR, Conn PJ. 1998. RGS4 inhibits signaling by group I metabotropic glutamate receptors. J Neurosci 18:905–913.

Sinnarajah S, Dessauer CW, Srikumar D, Chen J, Yuen J, Yilma S, Dennis JC, Morrison EE, Vodyanoy V, Kehrl JH. 2001. RGS2 regulates signal transduction in olfactory neurons by attenuating activation of adenylyl cyclase III. Nature 409:1051–1055.

Wilsch VW, Behnisch T, Jager T, Reymann KG, Balschun D. 1998. When are class I metabotropic glutamate receptors necessary for long-term potentiation? J Neurosci 18:6071–6080.